☙

Imaging the spontaneous formation of vortex-antivortex pairs in planar superconductor/ferromagnet hybrid structures

M. Iavarone,[1,2,3,*] A. Scarfato,[1,4,5] F. Bobba,[1,4,5] M. Longobardi,[1] G. Karapetrov,[3] V. Novosad,[3]
V. Yefremenko,[3] F. Giubileo,[4] and A. M. Cucolo[1,4,5]

[1]*Physics Department, Università degli Studi di Salerno, Via Ponte Don Melillo, I-84084 Fisciano, Italy*
[2]*Department of Physics, Temple University, Philadelphia, Pennsylvania 19122, USA*
[3]*Materials Science Division, Argonne National Laboratory, Argonne, Illinois 60439, USA*
[4]*CNR-SPIN Laboratory, Via Ponte Don Melillo, I-84084 Fisciano, Italy*
[5]*Nanomates, Research Centre for Nanomaterials and Nanotechnology, Università degli Studi di Salerno, I-84084 Fisciano, Italy*

Low-temperature magnetic force microscopy has been used to visualize spontaneous formation of vortex-antivortex pairs in hybrid ferromagnet/superconductor systems. Vortex-antivortex pairs are induced by the periodic stray field of the ferromagnet. We find general equilibrium conditions for which spontaneous vortex-antivortex pairs are formed during zero-field cooling of the hybrid ferromagnet/superconductor bilayers. Vortices can be generated by the ferromagnet domains in the absence of an external field and they are thermodynamically stable for values of the stray field and the period of the stripe magnetic domains that exceed a certain threshold.

I. INTRODUCTION

Vortices play an important role in many systems such as superconductors, superfluid Fermi systems, and neutron stars, to name a few. Very recently, vortex dipoles in a Bose-Einstein condensate have been created by using a laser beam,[1] in analogy with vortex-antivortex (V-AV) pairs formed in a superconducting thin film deposited on the top of ferromagnetic Co dots.[2,3] Theoretically, it has been shown that V-AV pairs can be stabilized in a Bose-Einstein condensate under a confinement potential[4] similar to streets of vortices-antivortices in classical viscous fluids.[5] Moreover, the possibility to control the generation rate and the trajectories of V-AV pairs by an in-plane magnetic dipole on top of a superconducting film has also been demonstrated theoretically.[6] Insight into the basic mechanisms of formation, annihilation, and dynamics of V-AV pairs is still lacking. The ability to control their behavior in each of the above-mentioned systems depends on establishing correlations of the behavior of vortex dipole structures across different systems.

We focus on the behavior of vortex dipoles in hybrid planar superconducting/ferromagnetic (S/F) heterostructures. We tuned the experimental parameters of the superconductor and the ferromagnet that make the formation of V-AV pairs in these systems favorable. The stray field of the ferromagnet plays the role of a confinement potential for vortices, induces spontaneous generation of V-AV pairs, and determines vortex dynamics. Several studies have focused on the confinement of vortices by magnetic domains in bulk S/F bilayers[7–9] or by magnetic nanoparticles or ferromagnetic dots deposited above the superconducting layer.[10–16] The planar structure of the samples used in this study, compared to structures where the superconducting layer is deposited on the top of magnetic dots, allows us to eliminate the effects on vortices due to the change in topography of the superconductor at the edge of the magnetic dots.

STM measurements performed on magnetically coupled Permalloy(Py)/NbSe$_2$ (single-crystal) bilayers[17] revealed that magnetic stripe domains induce vortex chain configurations

that are quite different from the ones observed in superconductor/normal metal (S/N) hybrids.[18] At low fields vortices form chain structures spaced by $d = 2w$, where w is the magnetic stripe width of the Py domains. No spontaneous V-AV pairs were observed in zero applied magnetic field. It has been predicted theoretically that V-AV pairs could be induced by out-of-plane ferromagnet magnetization[19,20] when certain geometrical conditions among the ferromagnet stripe domain width, superconducting penetration depth, and superconductor thickness are met. However, spontaneous V-AV pairs in planar S/F systems have not been observed so far. We carried out a low-temperature magnetic force microscopy (MFM) investigation on a set of Py/Nb bilayers with different Py as well as Nb thicknesses. The two layers S and F are only magnetically coupled since a thin oxide layer is placed in between. Low-temperature MFM allows direct visualization of vortices in superconductors in the regime of low applied magnetic fields with relative insensitivity to surface conditions. Moreover, this technique has the advantage over the STM technique[21] of being sensitive to the vortex polarity and magnetic domains in Py.

II. EXPERIMENTAL DETAILS

Py films were grown by dc sputtering on a Si substrate from a Fe$_{19}$Ni$_{21}$ target at a base pressure of 1.5×10^{-7} Torr, followed by a 10-nm SiO$_2$ layer. For some of the samples a SiN layer was used instead of a SiO$_2$ layer. SiN was deposited from a Si target in an Ar/N$_2$ 1:6 mixture. Nb films were grown by dc sputtering in a dedicated system at room temperature in a high vacuum ($P = 5.8 \times 10^{-9}$ Torr) at a deposition rate of 0.116 nm/s. The superconducting critical temperature was determined by superconducting quantum interference device (SQUID) magnetometry and measured in a small applied field ($H = 1$ Oe). Some of the bilayers were prepared for electrical transport measurements using photolithography to produce microbridge patterns 2.0 mm long and 5 μm wide. From transport measurements we obtained $-\mu_0 \frac{dH_{c2}}{dT}|_{T_c} = 0.27$ T/K, which yields a value of the coherence length $\xi_0 \approx 12$ nm. The

value of the penetration depth has been estimated using the dirty limit expressions as derived by Gor'kov:[22]

$$\lambda(0) = 1.63\kappa\xi(0) = 1.05 \times 10^{-3}\sqrt{\rho_0/T_c} \approx 61 \text{ nm}, \quad (1)$$

where κ is the Ginsburg-Landau parameter, $\rho_0 = 3 \times 10^{-8}$ Ω m is the residual resistivity and $T_c = 8.95$ K. This yields a value of the penetration depth at $T = 6$ K of $\lambda(6 \text{ K}) = \frac{\lambda(0)}{\sqrt{1-(T/T_c)^4}} \approx 68$ nm and a coherence length $\xi(6 \text{ K}) = \xi_0(\frac{T_c}{T_c-T})^{1/2} \approx 21$ nm.

In this work we study Py/Nb bilayers, focusing our attention on Nb films that are not thinner than 100 nm. Niobium has a very high solubility and binding energy for oxygen, and thus the structure and morphology of Nb surface are affected by this stage of oxidation. Scanning tunneling microscopy characterization of 100-nm-thick films of Nb revealed that the films form grains with a typical size of $20 \div 30$ nm. Several types of oxides that form on the surface film and penetrate the film through the grains weaken the superconductivity locally and serve as easy flux entry points. Deposition of capping overlayers does not change this morphology. The size of the Nb grains grows only by annealing the Nb film at a very high temperature.[23] This procedure, however, cannot be used in the case of Py/Nb bilayers due to the presence of the magnetic layer, which cannot be heated during fabrication and processing of the Nb layer. For this reason, we limit our study to Nb films thicker than 100 nm without any capping layer.

Permalloy is a ferromagnetic material in which the magnetic domain configuration can be controlled by the thickness. At thicknesses above a critical thickness $t_c = 2\pi\frac{A}{K_u}$, where $A = 1 \times 10^{-6}$ erg/cm is the exchange potential and K_u is the perpendicular anisotropy, has a well-ordered stripe domain structure.[24,25] The stripe width $w \propto \sqrt{t}$, where t is the Py film thickness. For our samples, magnetization hysteresis loops reveal a perpendicular anisotropy of $K_u \approx 6 \times 10^4$erg/cm^3 at $T = 10$ K, which yields a critical thickness of about 200 nm. The stray field of the periodic domains decays as a function of the distance from the Py surface as

$$H(z)$$
$$= \sum_{n=0}^{n=\infty} A_n \frac{(-1)^n}{2n+1} \sin\left(\frac{\pi}{w}(2n+1)x\right) \exp\left(-\frac{\pi}{w}(2n+1)z\right),$$
$$(2)$$

where w is the stripe's width and z is the distance from the Py surface.[25] Since the Curie temperature of the Py is higher than the superconducting temperature T_c of the Nb films, when the temperature is decreased below T_c the superconductor is field-cooled in a spatially nonuniform field.

III. RESULTS

MFM measurements were performed with an Omicron CryoSFM in frequency modulation MFM (FM-FMM) mode. The system uses fiber-optic interferometry to detect the cantilever deflection. The scanner is equipped with an *x-y* positioning system to allow scanning of different portions of the sample surface. During experiments the pressure in the measurement chamber is higher than 10^{-10} Torr. We used commercial low-moment ($<1 \times 10^{-13}$ emu) magnetic can-

tilevers (MESP-LM) from Veeco, with a resonant frequency of 85 kHz and an elastic constant of 2.8 N/m. In FM-MFM the tip is oscillated at its resonant frequency, while tip-sample interaction forces cause the resonant frequency to shift. MFM images are maps of the shifts in the cantilever resonant frequency df, recorded as a function of the position, while scanning the tip at a constant height from the sample's surface. All measurements presented here were performed by cooling through a superconducting T_c with a tip-sample distance of several tens of microns. This assures that the stray field of the tip does not influence the vortex distribution in the Nb films.

In Fig. 1 we report frequency shift maps recorded on the surface of three Py/Nb samples above and below the superconducting critical temperature of the samples. The three samples have the same thickness of Py (1 μm), and therefore the same domain width of 470 nm, as shown in Fig. 1. The oxide layer is 10 nm thick, while the Nb thicknesses are 100, 150, and 360 nm, respectively. Above the superconducting critical temperature T_c the stripe domains of the Py are observed through the Nb layer in the normal state. Below T_c, in zero applied magnetic field, the stripe domains of the Py are still clearly visible in samples with Nb thicknesses of 100 and 150 nm [Figs. 1(d) and 1(e)] but not visible in the sample with thicker Nb films [Fig. 1(f)]. Quantitative analysis of the MFM frequency shift maps could provide an estimate of the penetration depth of the Nb films, but the procedure is not straightforward and depends critically on the tip model used.[26] A qualitative estimate of λ from the df maps in MFM images above and below T_c yields values that are consistent with those inferred from transport measurements. Below T_c, in zero applied magnetic field, no spontaneous V-AV pairs were observed for these samples [Figs. 1(d)–1(f)].

We performed MFM measurements on reference Nb films deposited on a Si substrate and having the same thickness of the films in the F/S structures. Vortices could be induced in our reference Nb films in applied external fields as low as 5 Oe (much smaller than the stray field of the Py). This suggests that if the Py stray field is not sufficient to induce vortices in the same thickness Nb film, then the inhomogeneous field distribution in the superconductor is playing a major role in determining the flux quantization in S/F structures. Moreover, vortices can be induced in Py/Nb samples by field-cooling in an external applied magnetic field. In Fig. 2, two MFM images acquired at 5.7 K on a bilayer with 200 nm of Nb in an applied field of $H = -22$ Oe and $H = +18$ Oe are reported. In Fig. 2(a) the field in vortices is parallel to the tip magnetization, and thus it exhibits an attractive force, therefore vortices appear as darker regions in the image. Conversely, the vortices in Fig. 2(b) appear as brighter regions since the force is now repulsive, the field of the vortices and that of the tip being antiparallel. The vortex density is not homogeneous. The vortices created by the external field are preferentially pinned at stripes with the same polarity, as expected theoretically[28] and confirmed by STM experiments.[17] Moreover, vortices form a chain structure in the middle of the Py stripe domains. The distance between vortices is consistent with the applied magnetic field, with local deviations due to the Nb intrinsic pinning. Similar images have been observed in Py/Nb samples with 150- and 360-nm-thick Nb films and 1-μm-thick Py film.
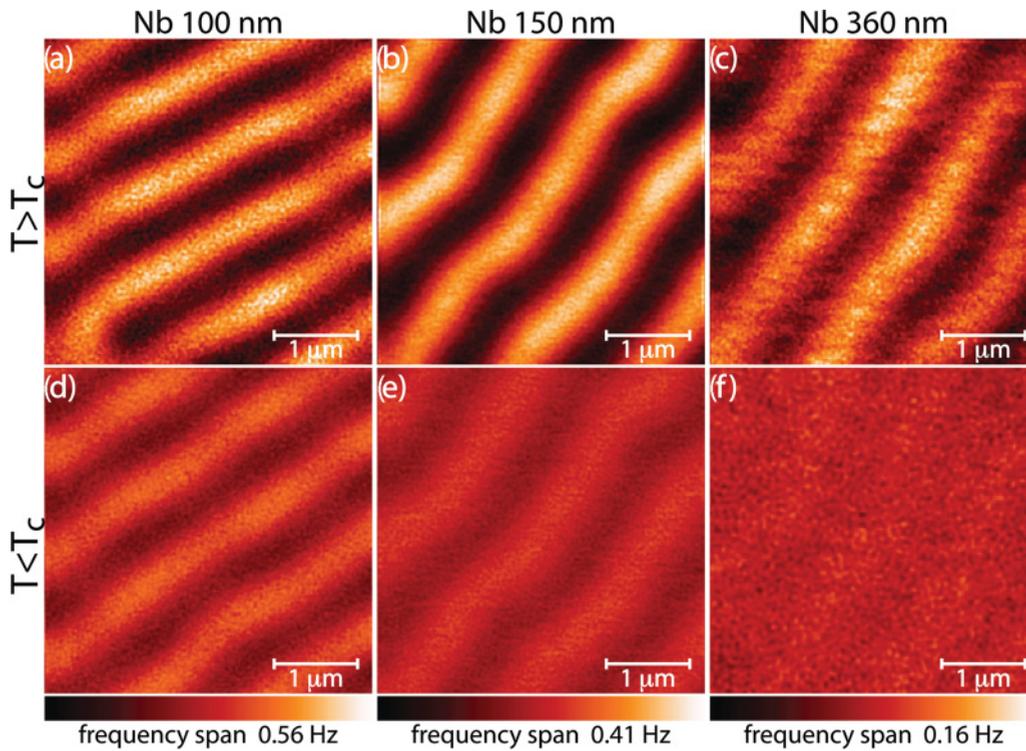
FIG. 1. (Color online) MFM frequency shift maps for three Py/Nb bilayers, magnetically coupled through a 10-nm layer of SiO_2. The thickness of the Py film is 1 μm for all samples. Nb thicknesses are (a, d) 100 nm, (b, e) 150 nm, and (c, f) 360 nm. Maps were acquired (a–c) at $T = 12$ K (above T_c) and (d–f) at $T = 6$ K (below T_c). The frequency span is (a, d) 0.56 Hz, (b, e) 0.41 Hz, and (c, f) 0.16 Hz. Images were obtained by scanning at heights of (a, b, d, e) $z = 100$ nm and (c, f) $z = 50$ nm. The scanning area is 3.5×3.5 μm in all images. For increasing Nb thickness, the distance between the tip and the Py increases, and consequently the stripes' magnetic contrast is consistently weaker even at temperatures higher than T_c.

The above experimental results demonstrate the key role played by the local field distribution in a superconducting film, determined by the superconducting thickness d_s, the penetration depth λ, and the Py stray field $H(x,y,z)$. Experimentally the parameters that can be tuned are the superconducting thickness d_s and the stripe domain width of the magnetic material. For the reasons discussed above related to the morphology of thinner Nb films and the effect on the flux penetration, we chose to tune the magnetic domain size. Py offers the opportunity to easily tune the stripe domain width,
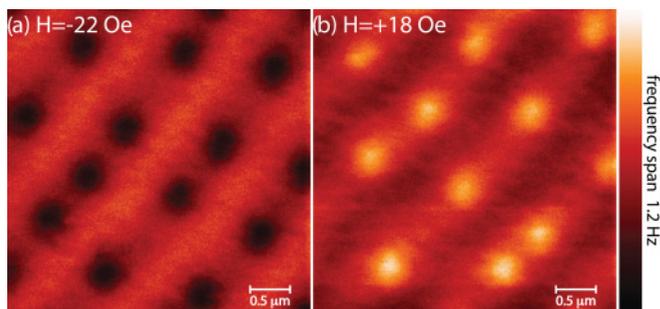
FIG. 2. (Color online) MFM images acquired at $T = 5.7$ K, at height $z = 60$ nm, from a Py/Nb (200-nm) bilayer for field-cooling in an applied field of (a) $H = -22$ Oe and (b) $H = +18$ Oe. The scanning area is 3.5×3.5 μm in both cases. The Py thickness is 1-μm and the oxide layer between Py and Nb is 10 nm of SiO_2.

and therefore the z dependence of the stray field, by changing its thickness. We fabricated and characterized Py/Nb bilayers with 4-μm-thick Py and 200-nm-thick Nb. For these samples we measured a stripe domain width of $w = 1.1$ μm and we did observe spontaneous formation of V-AV chains [Fig. 3(a)] occupying the center of stripes with the same polarity. The average vortex (or antivortex) density in Fig. 3(a) corresponds to a field of $H = 35$ Oe. V-AV pairs are stable at temperatures up to very close to T_c. The force between tip and sample is a function of the distance tip sample. The in-plane component of this force can be used to push or pull vortices.[27] By bringing the tip closer to the surface (to a distance of about $z = 10$ nm), we can estimate that the lateral force between tip and sample is about 4 pN. To move a vortex we bring the tip to a distance of about 10 nm and then scan parallel to the surface as many as several times, then we bring the tip back to $z > 100$ nm and scan again to see whether or not this induced changes in the vortex configuration. Forces of 4 pN, when normalized to a Nb thickness of 200 nm, correspond to 20 pN/μm. We could neither depin nor annihilate V-AV pairs by applying forces of up to 20 pN/μm at $T = 8.7$ K along and perpendicular to the stripe domains.

If an external magnetic field is applied during the cooling process, one type of magnetic domain is partially compensated and the relative density of vortices and antivortices is changed as shown in Fig. 3(b). In the regions with a higher vortex
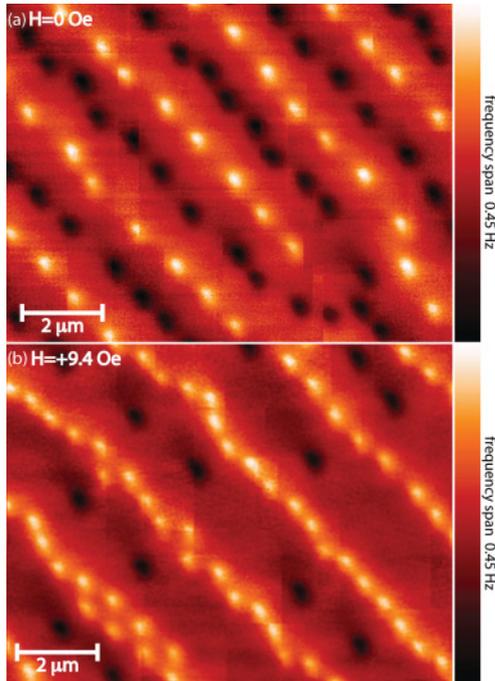
FIG. 3. (Color online) MFM images acquired on a Py/Nb bilayer magnetically coupled through a 10-nm layer of SiN. The thickness of Py is 4 μm; that of the Nb film, 200 nm; and the stripe's width is 1.1 μm. (a) Zero-field-cooled image showing V-AV pairs spontaneously created by the stray field of the Py. (b) Field-cooled image obtained in an external applied field of $H = +9.4$Oe. Images were obtained by scanning at a constant height $z = 60$ nm and a temperature $T = 5.7$ K. The scanning area for both images is 11.4×8.7 μm^2.

density we can clearly see the switching from one to two chains in a zigzag configuration.

IV. DISCUSSION

The theoretical description of the S/F hybrid structure has to take into account the stray field $H(x,y,z)$ produced by the ferromagnet. The condition for spontaneous formation of V-AV pairs in S/F hybrids has been considered theoretically in Refs. 19 and 20 in the case of a ferromagnet with out-of-plane magnetization forming alternating up and down domains $\pm M_0$ along one of the in-plane axes. This simplified model is sufficient to describe the effect of the out-of-plane component of the Py stray field on vortices in a superconducting Nb film. Indeed, since Nb is a three-dimensional (3D) superconductor, any in-plane component of Py magnetization is not expected to affect the vortex lattice. In such S/F systems the spontaneous formation of V-AV pairs in the superconductor becomes advantageous when the energy of the system with vortices becomes lower than that of a vortex-free system. The total energy of the S/F system is given by $E_{\text{TOT}} = E_{\text{SV}} + E_{\text{VV}} + E_{\text{VM}} + E_{\text{MM}} + E_{\text{DW}}$, where E_{SV} is the self-energy of the single vortex, E_{VV} is the vortex-vortex interaction energy, E_{VM} is the interaction energy between the vortices and the magnetic field of the ferromagnet, E_{MM} is the self-energy of the ferromagnet, and E_{DW} is the surface energy of the domain walls. The energy term E_{VV} can be

neglected in the approximation of a low vortex density. The ferromagnet self-energy E_{MM} and the domain wall surface energy E_{DW} are relevant to determine the magnetic domain structure at equilibrium, and therefore they can be neglected. This brings us to the condition for spontaneous formation of V-AV pairs, $E_{\text{TOT}} \approx E_{\text{SV}} + E_{\text{VM}} < 0$. A general expression for the minimization of the total energy of the system has been obtained and can be solved numerically. The limit cases of thick and thin superconducting films (compared to the penetration depth λ) have been obtained in Refs. 20 and 19, respectively. Additional contributions to the total energy in the general formula are at least 1 order of magnitude smaller than the contributions considered in the limit cases. The final expressions depend strongly on the ratio of the domain width to the thickness of the superconducting layer. In the limit of thick superconducting films, $d_s > \lambda$ (where d_s is the superconducting film thickness), and stripe domain widths larger than λ ($w \gg \lambda$), the self-energy of a single vortex is

$$E_{\text{SV}} = \frac{\Phi_0^2 d_s}{16\pi^2\lambda^2} ln\frac{\lambda}{\xi} \qquad (3)$$

and

$$E_{\text{VM}} \approx -4M_0\Phi_0 w \frac{0.916}{\pi^2}. \qquad (4)$$

Therefore, vortices will be energetically favorable only if M_0 is larger than a critical value,

$$M_0 > \frac{\Phi_0}{64\lambda^2}\frac{d_s}{0.916w}ln\frac{\lambda}{\xi} \approx 0.2\frac{d_s}{w}H_{c1}, \qquad (5)$$

where $H_{c1} = \frac{\Phi_0}{4\pi\lambda^2}ln\frac{\lambda}{\xi}$ is the lower critical field of the superconductor. The local out-of-plane magnetization of Py cannot be easily measured directly. From measurements of the upper critical field of S/Py bilayers and Py/S/Py trilayers,[30] we can estimate the stray field to be of the order of 80 Oe at 50 nm from the Py surface, which corresponds to a value of $M_0 \approx$ 16 G. Micromagnetic simulation of 1μm- and 4-μm-thick Py films, using saturation magnetization and uniaxial anisotropy derived from magnetization hysteresis measurements, yield similar 2D magnetization and stray field profiles and values. According to the above criterion, samples with stripe width $w \approx 470$ nm do not satisfy the condition for spontaneous formation of V-AV pairs if $d_s > 90$ nm. In samples with wider stripe domains, $w = 1100$ nm, instead, V-AV pairs should be formed at thicknesses $d_s < 210$ nm, in agreement with the observation of spontaneous formation of V-AV pairs only in Py/Nb samples with 4-μm-thick Py and 200-nm-thick Nb.

It is important to note that in the presence of an external magnetic field H, there is an additional energy contribution $\pm Hd_s\Phi_0/4\pi$, with the sign depending on the mutual orientation of the applied field and vorticity. As a result, inside the domains, where the external magnetic field compensates the field of the domain, the number of vortices will decrease, and eventually they will disappear at $H \simeq 4\pi|E_{\text{tot}}|/(d_s\Phi_0)$. We imaged the vortex configuration at different values of the applied magnetic field, at low values of the field, in the field-cooling process. We clearly observed that the relative population of vortices and antivortices changes gradually according to the applied field. However, this does not allow

us to draw exact quantitative conclusions since the number of vortices in the scanning area is too low. When vortices are too far apart we do not have any statistically reliable information about the average distance between vortices. Also, we should note that the density of spontaneously generated V-AV pairs [Fig. 3(a)] is slightly lower than that expected for a given value of the stray field above the stripe domains. This is due to the growing relevance of the neglected vortex-vortex interaction term E_{VV} when the distance between the vortices is of the order of λ as well as the partial screening of the magnetic field by the Meissner currents flowing above the magnetic domain walls.

In conclusion, we have confirmed experimentally the criterion for spontaneous formation of V-AV pairs in planar F/S hybrids by tuning of the magnetic domain stripe width. The spontaneously generated V-AV pairs are thermodynamically stable and strongly pinned. The key role for formation of

V-AV is played by the out-of-plane magnetization of the ferromagnet and by the ratio of the magnetic domain width to the superconducting film thickness.

*Corresponding author. iavarone@temple.edu

[1] T. W. Neely, E. C. Samson, A. S. Bradley, M. J. Davis, and B. P. Anderson, Phys. Rev. Lett. **104**, 160401 (2010).

[2] M. J. Van Bael, J. Bekaert, K. Temst, L. Van Look, V. V. Moshchalkov, Y. Bruynseraede, G. D. Howells, A. N. Grigorenko, S. J. Bending, and G. Borghs, Phys. Rev. Lett. **86**, 155 (2001).

[3] J. S. Neal, M. V. Miloševic, S. J. Bending, A. Potenza, L. San Emeterio, and C. H. Marrows, Phys. Rev. Lett. **99**, 127001 (2007).

[4] K. Sasaki, N. Suzuki, and H. Saito, Phys. Rev. Lett. **104**, 150404 (2010).

[5] C. H. K. Williamson Annu. Rev. Fluid Mech. **28**, 477 (1996).

[6] V. N. Gladilin, J. Tempere, J. T. Devreese, W. Gillijns, and V. V. Moshchalkov, Phys. Rev. B **80**, 054503 (2009).

[7] L. N. Bulaevskii, E. M. Chudnovsky, and M. P. Maley, Appl. Phys. Lett. **76**, 2594 (2000).

[8] Yu. I. Bespyatykh and W. Wasilevski, Phys. Solid State **43**, 224 (2001).

[9] A. A. García-Santiago, F. Sánchez, M. Varela, and J. Tejada, Appl. Phys. Lett. **77**, 2900 (2000).

[10] M. J. Van Bael, J. Bekaert, K. Temst, L. Van Look, V. V. Moshchalkov, Y. Bruynseraede, G. D. Howells, A. N. Grigorenko, S. J. Bending, and G. Borghs, Phys. Rev. Lett. **86**, 155 (2001).

[11] Y. Jaccard, J. I. Martín, M. C. Cyrille, M. Vélez, I. K. Schuller, and J. L. Vicent, Phys. Rev. B **58**, 8232 (1998).

[12] J. I. Martín, M. Vélez, A. Hoffmann, J. L. Vicent, and I. K. Schuller, Phys. Rev. Lett. **83**, 1022 (1999).

[13] A. Terentiev, D. B. Watkins, L. E. De Long, L. D. Cooley, D. J. Morgan, and J. B. Ketterson, Phys. Rev. B **61**, R9249 (2000).

[14] O. M. Stoll, M. I. Montero, J. Guimpel, J. J. Akerman, and I. K. Schuller, Phys. Rev. B **65**, 104518 (2002).

[15] Q. H. Chen, G. Teniers, B. B. Jin, and V. V. Moshchalkov, Phys. Rev. B **73**, 014506 (2006).

[16] T. Shapoval, V. Metlushko, M. Wolf, B. Holzapfel, V. Neu, and L. Schultz, Phys. Rev. B **81**, 092505 (2010).

[17] G. Karapetrov, M. V. Miloševic, M. Iavarone, J. Fedor, A. Belkin, V. Novosad, and F. M. Peeters, Phys. Rev. B **80**, 180506 (2009).

[18] G. Karapetrov, J. Fedor, M. Iavarone, D. Rosenmann, and W. K. Kwok, Phys. Rev. Lett. **95**, 167002 (2005).

[19] G. M. Genkin, V. V. Skuzovatkin, and I. D. Tokman, J. Mag. Mat. **130**, 51 (1994).

[20] R. Laiho, E. Lähderanta, E. B. Sonin, and K. B. Traito, Phys. Rev. B **67**, 144522 (2003).

[21] A. Kohen, T. Cren, T. Proslier, Y. Noat, W. Sacks, D. Roditchev, F. Giubileo, F. Bobba, A. M. Cucolo, N. Zhigadlo, S. M. Kazakov, and J. Karpinski, Appl. Phys. Lett. **86**, 212503 (2005).

[22] L. P. Gor'kov, Zh. Eksp. Teor. Fiz. **36**, 1918 (1959) [Sov. Phys. JETP **9**, 1364 (1959)] ; P. H. Kes and C. C. Tsuei, Phys. Rev. B **28**, 5126 (1983).

[23] B. An, S. Fukuyama, K. Yokogawa, and M. Yoshimura, Phys. Rev. B **68**, 115423 (2003).

[24] Y. Murayama, J. Phys. Soc. Jpn. **21**, 2253 (1966).

[25] S. Chikazumi, *Physics of Ferromagnetism* (Oxford University Press, New York, 1997).

[26] U. Hartmann, Annual Review of Materials Science **29**, 53 (1999).

[27] E. W. Straver, J. E. Hoffman, O. M. Auslanender, D. Rugar, and K. A. Moler, Appl. Phys. Lett. **93**, 172514 (2008).

[28] S. Erdin, I. F. Lyuksyutov, V. L. Pokrovsky, and V. M. Vinokur, Phys. Rev. Lett. **88**, 017001 (2001).

[29] G. Carneiro and E. H. Brandt, Phys. Rev. B **61**, 6370 (2000).

[30] A. Belkin, V. Novosad, M. Iavarone, J. Fedor, J. E. Pearson, A. Petrean-Troncalli, and G. Karapetrov, Appl. Phys. Lett. **93**, 072507 (2008); A. Belkin, V. Novosad, M. Iavarone, R. Divan, J. Hiller, T. Proslier, J. E. Pearson, and G. Karapetrov, *ibid.* **96**, 092513 (2010).